Carbohydrate Polymers 85 (2011) 733–737

Contents lists available at ScienceDirect

Carbohydrate Polymers

journal homepage: www.elsevier.com/locate/carbpol

Formation of hydrogels from cellulose nanofibers

Kentaro Abe[a,b,*], Hiroyuki Yano[a,b]

[a] Pioneering Research Unit for Next Generation, Kyoto University, Gokasyo, Uji, Kyoto 611-0011, Japan
[b] Research Institute for Sustainable Humanosphere, Kyoto University, Gokasyo, Uji, Kyoto 611-0011, Japan

ARTICLE INFO

Article history:
Received 6 January 2011
Received in revised form 1 March 2011
Accepted 15 March 2011
Available online 9 April 2011

Keywords:
Hydrogel
Cellulose nanofiber
Alkaline treatment

ABSTRACT

We report the preparation of hydrogels from an aqueous suspension of crystalline cellulose nanofibers only by alkaline treatment. The nanofiber suspensions were converted into two kinds of hydrogels with different crystal forms in response to the increasing concentration of sodium hydroxide (NaOH). When treated in 6–9 wt% NaOH, a hydrogel was formed by aggregating the nanofibers with the original morphology and the original crystal form, cellulose I. However, the hydrogel prepared at 15 wt% NaOH had a network formed by the coalescence of cellulose nanofibers and exhibited a highly crystalline cellulose II structure. This gelation process seems to be caused by the axial shrinkage of the cellulose nanofibers in aqueous alkaline solutions.

1. Introduction

Plant cell walls have a strong framework or scaffold consisting of nano-scale crystalline bundles of cellulose molecules, called microfibrils. Because of the stable structure provided mainly by inter/intramolecular hydrogen bonds, the crystal region displays strong mechanical properties longitudinally, e.g., 138 GPa of the elastic modulus (Sakurada, Nukushima, & Ito, 1962) and 0.6×10^{-5}/K of the thermal expansion coefficient (Hori & Wada, 2005). In addition to these properties, because of their low weight and morphological features such as large specific surface areas and high aspect ratios, plant-based cellulose nanofibers have great potential for reinforcing polymer matrices.

A variety of fibrillation methods using mechanical treatment have been reported for the preparation of cellulose nanofibers, and currently nanofibers can be isolated from various plant sources (Siró & Plackett, 2010). We have also reported an isolation method in which plant fibers are ground in an undried state, and have prepared cellulose nanofibers from various sources such as softwood, rice straw, potato tuber and bamboo (Abe, Iwamoto, & Yano, 2007; Abe & Yano, 2009, 2010). In our previous study, a wood sample was homogeneously fibrillated by just one-time grinding, and the resultant nanofibers had a uniform width of approximately 15 nm and a length of more than several micrometers (Abe et al., 2007). The uniformity was emphasized by the fact that the nanofibers homogeneously dispersed in water without aggregation and sedimentation. Moreover, the suspension exhibited a very high viscosity even with 1 wt% nanofiber because of the large hydrophilic surface area and entanglement (Abe et al., 2007; Pääkkö et al., 2007).

In this manner, the homogeneous cellulose nanofibers behaved in water like dissolved polymers while maintaining good crystallinity at the same time. This study focused on the unique properties of nanofiber suspension and prepared the hydrogels based on cellulose nanofibers by soaking in alkaline aqueous solutions and then neutralization. In the present study, we investigated the physical and structural characteristics of nanofiber-based hydrogels prepared with various concentrations of alkaline solutions and here discuss the gelation behavior of cellulose nanofibers.

2. Experimental

2.1. Materials

The raw material for cellulose nanofiber was wood powder from Hinoki cypress (*Chamaecyparis obtusa*) sieved under 60 mesh. The sample was dewaxed in a Soxhlet apparatus with a 2:1 (v/v) mixture of toluene/ethanol for 6 h, and then air-dried and stored at room temperature.

2.2. Purification and isolation of cellulose nanofibers

The procedure basically followed the method we used in previous studies (Abe et al., 2007; Abe & Yano, 2009, 2010). Wood powder was purified by a series of chemical treatments as follows. First, the lignin in the sample was removed using an acidified sodium chlorite solution at 70 °C for 5 h, according to the method by

---

[*] Corresponding author at: Pioneering Research Unit for Next Generation, Kyoto University, Gokasyo, Uji, Kyoto 611-0011, Japan. Tel.: +81 774 383 658; fax: +81 774 383 655.
E-mail address: abekentaro@rish.kyoto-u.ac.jp (K. Abe).

0144-8617/$ – see front matter © 2011 Elsevier Ltd. All rights reserved.
doi:10.1016/j.carbpol.2011.03.028

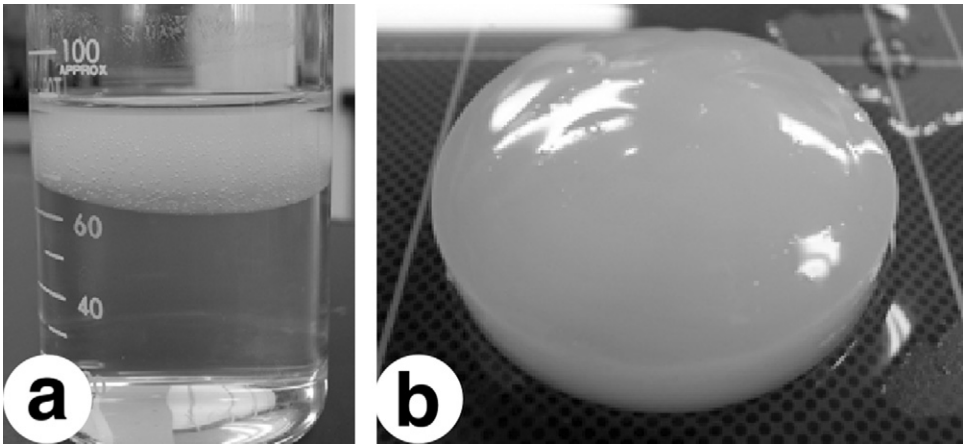

Fig. 1. Nanofiber suspension in aqueous NaOH solution (a) and hydrogel obtained after treatment at 9 wt% NaOH and neutralization (b).

Wise, Murphy and D'Addieco (1946). The sample was then treated in 5 wt% potassium hydroxide at 80 °C for 2 h to remove mainly hemicelluloses. After each chemical treatment, the sample was filtered and rinsed with distilled water until the residues were neutralized. The α-cellulose content of the purified sample was approximately 85% when determined by extraction with 17.5 wt% NaOH.

The undried purified sample was suspended in distilled water (1 wt%) and passed once through a grinder (MKCA6-3; Masuko Sangyo Co., Ltd., Saitama, Japan) at 1500 rpm. The grinding treatment was performed with a clearance gauge of −6 (corresponding to a 0.6 mm shift) from a zero position. This treatment allowed us to obtain an aqueous suspension of cellulose nanofibers.

2.3. Preparation of hydrogels

The nanofiber suspension was diluted with water into 0.8 wt%. The suspensions (20 g) were placed in a beaker so that the surface became as flat as possible. Alkali solutions (80 g) with five different amounts of sodium hydroxide (6, 9, 12, 15 and 21 g) were then carefully and slowly poured into the beaker so as not to deform the shape of the suspension. The beakers were kept at two temperatures, 20 °C and 50 °C, for 12 h. The equilibrium was confirmed using a digital sodium hydroxide refractometer (PAL-40S, Atago Corp.), and the concentrations reached 6, 9, 12, 15 and 21 wt%, respectively. The initial and equilibrium concentrations of NaOH aqueous solutions are listed in Table 1. Afterward, the samples in the semi-gel state were completely neutralized into beakers containing 4% dilute acetic acid for 6 h and then rinsed under running water for 12 h.

2.4. Characterization of cellulose nanofiber-based hydrogels

2.4.1. Measurements of shrinkage and nanofiber content

The dimensional changes with alkaline treatments were determined by the inner diameter (40.6 mm) of the beaker and the diameter of the obtained hydrogels, measured with a caliper. The nanofiber content in the hydrogels was calculated by measuring the weights of the hydrogels and the oven-dried one.

Table 1
Initial and equilibrium concerntrations of NaOH aqueous solution for the preparation of the hydrogels.

Initial (wt%)	Equilibrium (wt%)
7.5	6
11.25	9
15	12
18.75	15
26.25	21

2.4.2. X-ray diffraction

The hydrogels were slowly hot-pressed at 120 °C into sheets 1 mm in thickness and then subjected to X-ray diffraction measurement by the transmission method. Equatorial diffraction patterns were obtained by an X-ray generator (UltraX 18HF; Rigaku Corp., Tokyo, Japan) with CuKα radiation (40 kV and 250 mA) from 5° to 40°.

2.4.3. Field-emission scanning electron microscope (FE-SEM)

Hydrogels of less than 1 mm in thickness were prepared in order to avoid incorrect observations by a difference in alkaline concentrations between the initial state and the equilibrium state. A drop (0.1 g) of the nanofiber suspension with 0.8 wt% was placed in a beaker, and 300 ml of each alkali solution with 9 wt% and 15 wt% NaOH was carefully poured. The subsequent process was the same as that previously described, but the temperature was only 50 °C. The thin hydrogels were dehydrated through an ethanol series (50, 60, 70, 80, 90, 95, 100, 100%, 15 min each), replaced by t-butanol (30 min), and finally freeze-dried. The samples were coated with platinum by an ion sputter coater and then observed with a FE-SEM (JSM-6700F; JEOL Ltd., Tokyo, Japan) operating at 1.5 kV.

3. Results and discussion

3.1. Gelation of cellulose nanofiber

The suspension with 0.8 wt% nanofiber exhibited a high viscosity but still possessed fluidity. Immediately after the NaOH aqueous solutions were added, the suspensions were floated on top of the solutions regardless of the NaOH concentration (Fig. 1a) and then gradually shrank as mutual diffusion took place between the two phases. In the NaOH concentration range examined in this study, the hydrogels were obtained after neutralization; they had no fluidity and maintained their shape (Fig. 1b). None of the hydrogels reverted back to single nanofibers in water, and those obtained above 9 wt% could be readily handled by hand. As shown in Fig. 2, the diameter shrinkage of the hydrogels increased with an increasing NaOH concentration, and the nanofiber content thereby also increased. Both were drastically changed from 9 wt% to 15 wt%, and then leveled off above 15 wt%. Moreover, during the transition period, the turbidity and texture also changed. While the hydrogels prepared below 9 wt% looked like jelly with a little translucence, those prepared above 15 wt% became milky white and tougher in comparison. Concerning the effect of temperature, the hydro-

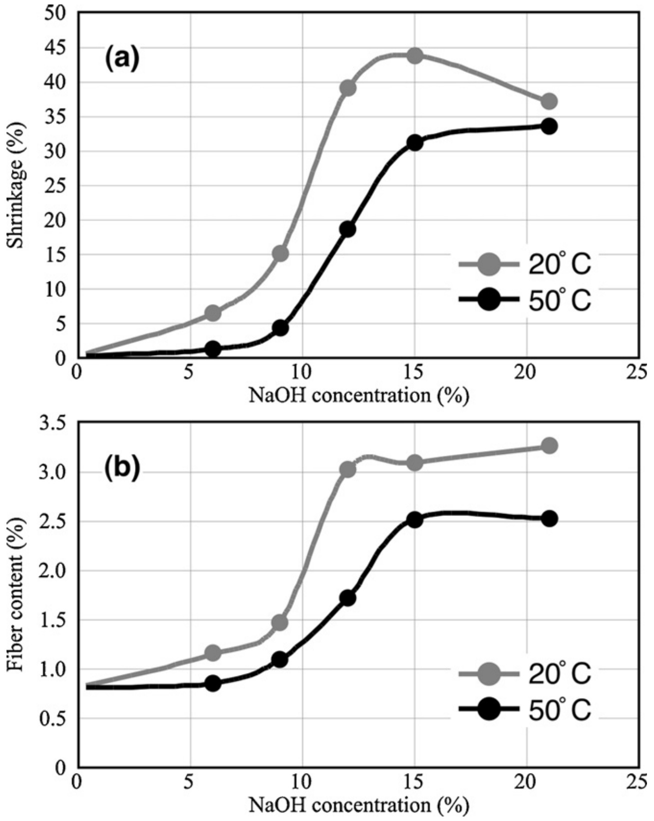

Fig. 2. Diameter shrinkage (a) and nanofiber content (b) of the hydrogels prepared at different NaOH concentrations.

gels prepared at 20 °C shrank more than those prepared at 50 °C, resulting in higher nanofiber contents.

3.2. *X-ray diffraction*

It is well known that native cellulose (cellulose I) is mercerized and converted into another crystal form (cellulose II) by soaking in strong alkaline solutions, washing with water and then drying. The X-ray diffraction patterns in Fig. 3 show the transition processes in the crystal structure of the dry matter of the hydrogel when the equilibrium concentrations of NaOH are increased. When the dry matter is prepared below 9 wt% NaOH, the X-ray patterns represent typical cellulose I regardless of temperature, although slight shoulders at approximately 13°were observed. However, at 12 wt% NaOH, the peaks specific to cellulose II at 2θ angles of approximately 12.3° and 20° appear with the patterns of cellulose I. Also, the hydrogel prepared at 20 °C was observed to have higher intensities of cellulose II than that prepared at 50 °C. Above 15 wt%, the crystal form was completely converted into cellulose II, but the hydrogel prepared at 20 °C showed lower crystallinity than that prepared at 50 °C.

3.3. *FE-SEM observations*

The X-ray results in Fig. 3 indicated the existence of two kinds of hydrogels having different crystal forms. To investigate these morphological features, FE-SEM observations were conducted on thin hydrogels, which were prepared in a large volume of alkaline solutions with 9 wt% and 15 wt% NaOH at 50 °C. This allowed us to minimize the difference between the initial and equilibrium concentrations. The samples were solvent-exchanged and then freeze dried to prevent structural collapse during dehydration.

At a low (1000×) magnification, both samples formed similar three-dimensional network structures with micro- and nanopores (Fig. 4a and d). However, the observation at higher magnifications demonstrated a structural difference between the hydrogel prepared at 9 wt% and that prepared at 15 wt% NaOH. In the hydrogel prepared at 9 wt% NaOH, Fig. 4b and c shows that the network was formed by the aggregation of individual cellulose nanofibers, which were very similar to those isolated from wood as shown in our previous study (Abe et al., 2007). On the other hand, in the case of 15 wt% NaOH, the nanofibers seem to become kinky and their aggregates form a network structure (Fig. 4e and f). Fig. 4 g in particular, at a magnification of 20,000 times, emphasizes the sponge-like structure formed via the coalescence of the kinky nanofibers.

We can summarize the results of the gelation of cellulose nanofibers as follows. In the 6–9 wt% NaOH solutions, the water suspension of cellulose nanofibers lost fluidity with a slight shrinkage. The hydrogel was easily obtained by subsequent neutralization, and the network was formed by aggregating the nanofibers with the original morphology and the original crystal form (cellulose I). The shrinkage of the suspension was significantly enhanced at around 12 wt% NaOH and then almost leveled off above 15 wt% NaOH. The hydrogel prepared at 15 wt% NaOH had a network structure with a sponge-like agglomeration and exhibited the cellulose II structure. As a result, we obtained two kinds of crystalline nanofiber-based hydrogels with different structures and crystal forms. The gelation mechanism of the cellulose nanofibers in alkaline solutions is discussed in the following.

Some studies have reported the behavior of fibrillated cellulose fibers during alkaline treatment (or mercerization). Dinand, Vignon, Chanzy, and Heux (2002) and Shibazaki, Kuga, and Okano (1997) prepared aqueous suspensions of fibrillated fibers using a homogenizer from never-dried bacterial cellulose and sugar beet pulp, respectively, and then subjected them to alkaline treatment with various concentrations of NaOH. In all of these studies, it was found that the fibrillated cellulose fibers were mercerized and irregularly aggregated when treated with 10–12 wt% NaOH. Therefore, the gelation mechanism in this study is based on similar aggregation behavior. In our case, the fabrication of the solid hydrogels can be accomplished because the individual cellulose nanofibers, which were isolated in this study, were homogeneously dispersed in water and then aggregated.

How are cellulose nanofibers aggregated and formed into hydrogels in alkaline solutions? The nonlinear increase of the shrinkage around 12 wt% NaOH in Fig. 2a suggests that salt-induced aggregation and shrinkage during osmotic dehydration are not the main reasons for the aggregation of cellulose nanofibers. One possibility is the longitudinal shrinkage of cellulose nanofibers during alkaline treatments. Previous studies support this possibility, and reported that the strong alkali treatment (mercerization) caused the longitudinal contraction of wood samples (Ishikura & Nakano, 2007; Nakano, Sugiyama, & Norimoto, 2000) and the in-plane contraction of cellulose samples, including a wet sheet of bacterial cellulose (Shibazaki et al., 1997) and a dry sheet of microfibrillated cellulose (Nakagaito & Yano, 2008). As an explanation for these behaviors, Nakano et al. proposed that the contraction is related to the entropy elastic force of cellulose microfibrils (Nakano, 2010; Nakano et al., 2000). Because the cellulose nanofiber isolated in this study corresponds to the cellulose microfibril aggregates (or bundles) in wood cell walls (Donaldson, 2007; Fahlén & Salmén, 2005; Tarashima et al., 2010), their proposal may be applied to our example. In fact, the observations when treated with 15 wt% NaOH indicated that the kinky structure is likely due to the shrinkage of the cellulose nanofibers, as shown in Fig. 4e–g. It is interesting to note, however, that the hydrogels could be formed even at NaOH concentrations below the mercerization threshold. This result suggests that even low NaOH concentrations cause some shrinkage of the cellulose

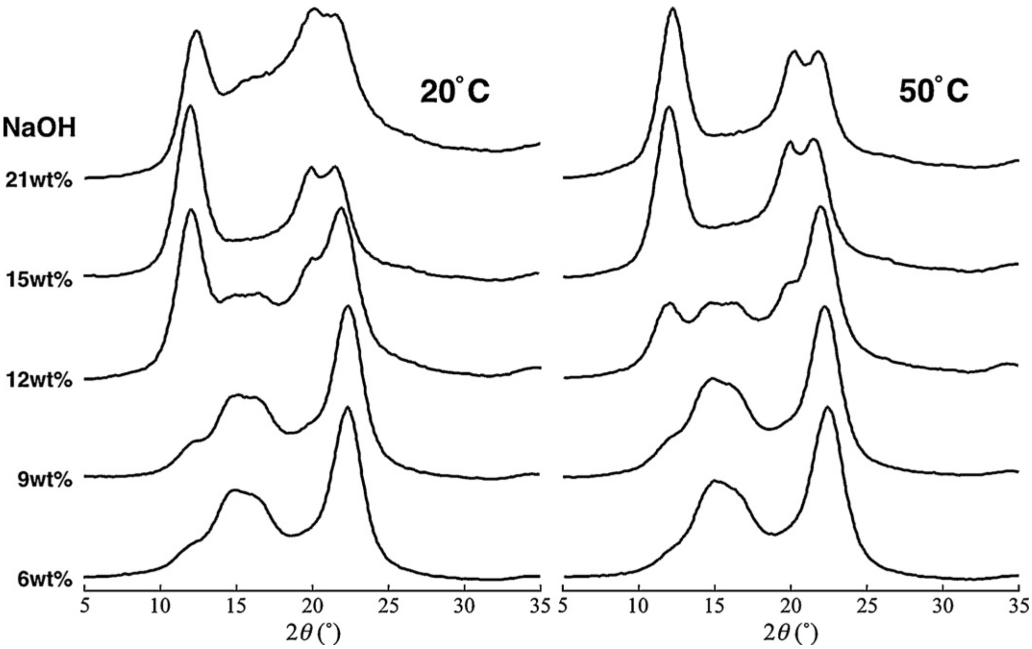

Fig. 3. Equatorial X-ray diffraction profiles of dried hydrogels prepared at different NaOH concentrations and at two temperatures, 20 °C (left) and 50 °C (right).

nanofibers with slight swelling, thus increasing the entanglement among nanofibers.

Based on the assumption that cellulose nanofibers longitudinally shrink in response to the increasing concentration of NaOH, we propose that these fibers have a certain nature for gel formation. At low NaOH concentrations before mercerization, the cellulose nanofibers slightly shrink and then a hydrogel, consisting of the original nanofibers with the crystal form of cellulose I, is formed via the enhancement of entanglement and aggregation. Around 12 wt% NaOH, the rate of entanglement is increased with the drastic shrinkage, and then the swelling nanofibers coalesce with each other at the contact points. At this time, it is likely that the antiparallel chain structure is partially formed by the interdigitation mechanism (Nishimura & Sarko, 1987; Okano & Sarko, 1985; Revol, Dietrich, & Goring, 1987) and the folding of the nanofiber itself (Kuga, Takagi, & Brown, 1993; Shibazaki et al., 1997). Because the nanofibers gradually approach as the NaOH concentration increases, the coalescence is accelerated and the system becomes stable above 15 wt% NaOH. After neutralization, the hydrogel obtained becomes tougher due to the irreversible mutual coalescence of the nanofibers, and the crystal form exhibits cellulose II in the dry state. However, before drying, a water-swollen hydrogel probably has the crystal structure of the cellulose II hydrate (Nishimura & Sarko, 1991; Wada, Ike, & Tokuyasu, 2010). Finally, the X-ray results in Fig. 3 suggest that,

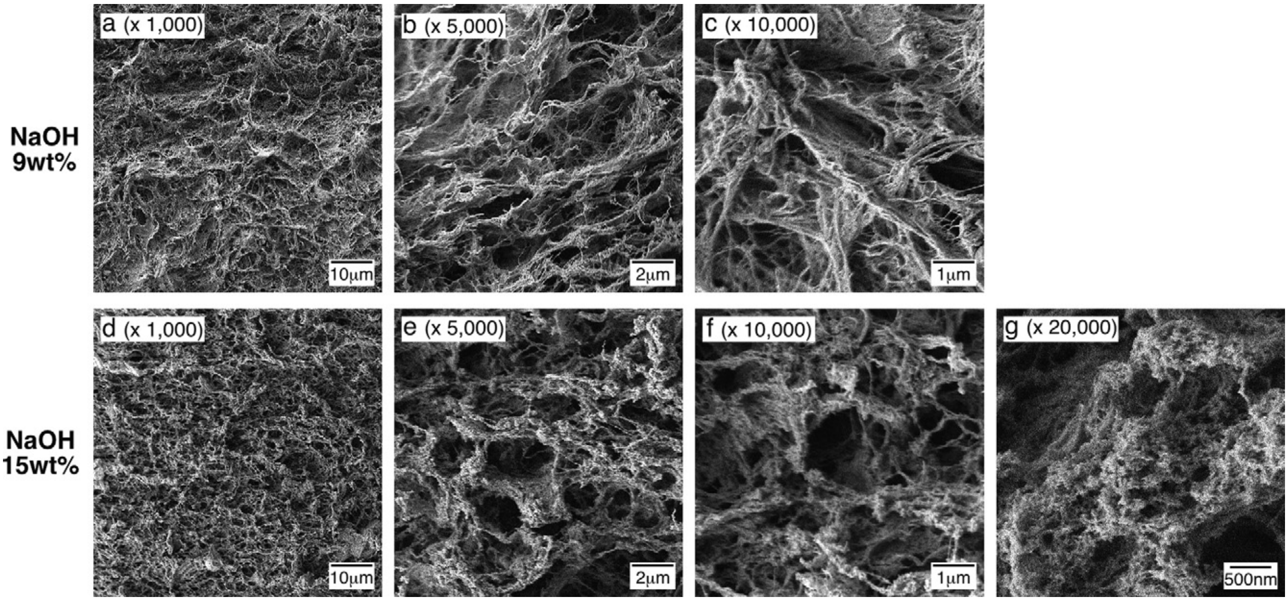

Fig. 4. FE-SEM micrographs of freeze-dried hydrogels prepared at 9 wt% NaOH (a–c) and 15 wt% NaOH (d–g).

when treated above 12 wt% NaOH, cellulose nanofibers partially dissolve even at 20 °C, resulting in low crystallinity.

4. Conclusions

In summary, cellulose nanofiber formed into crystalline hydrogels only by contacting aqueous NaOH solutions followed by neutralization. The two types of hydrogels with different crystal forms—celluloses I and II—were formed below and above the NaOH concentrations of approximately 12 wt%, respectively. FE-SEM observations showed that both of the hydrogels had consisting of the uniform nanofibers without any thicker fibrils. However, while the cellulose I-type hydrogel was formed by the entanglement of original nanofibers, the cellulose II-type hydrogel had a network formed by the coalescence of cellulose nanofibers via mercerization. At this point, we speculate that the main driving force for the gelation is probably the longitudinal shrinkage of the cellulose nanofibers in aqueous alkaline solutions. In this regard, future studies should further examine the behavior of cellulose microfibrils in aqueous alkaline solutions using isolated cellulose nanofibers.

Unlike conventional polymer hydrogels, the network of hydrogels prepared in this study consisted of crystalline nanofibers without dissolving. As a next step, our work will focus on evaluating and comparing the mechanical properties of the cellulose nanofiber-based hydrogels with two crystal forms with those of the hydrogels prepared from cellulose solutions.

References

Abe, K., Iwamoto, S., & Yano, H. (2007). Obtaining cellulose nanofibers with a uniform width of 15 nm from wood. *Biomacromolecules*, *8*, 3276–3278.

Abe, K., & Yano, H. (2009). Comparison of the characteristics of cellulose microfibril aggregates of wood, rice straw and potato tuber. *Cellulose*, *16*, 1017–1023.

Abe, K., & Yano, H. (2010). Comparison of the characteristics of cellulose microfibril aggregates isolated from fiber and parenchyma cells of Moso bamboo (*Phyllostachys pubescens*). *Cellulose*, *17*, 271–277.

Dinand, E., Vignon, M., Chanzy, H., & Heux, L. (2002). Mercerization of primary wall cellulose and its implication for the conversion of cellulose I→cellulose II. *Cellulose*, *9*, 7–18.

Donaldson, L. (2007). Cellulose microfibril aggregates and their size variation with cell wall type. *Wood Science and Technology*, *41*, 443–460.

Fahlén, J., & Salmén, L. (2005). Pore and matrix distribution in the fiber wall revealed by atomic force microscopy and image analysis. *Biomacromolecules*, *6*, 433–438.

Hori, R., & Wada, M. (2005). The thermal expansion of wood cellulose crystals. *Cellulose*, *12*, 479–484.

Ishikura, Y., & Nakano, T. (2007). Contraction of the microfibrils of wood treated with aqueous NaOH: evidence from changes in the anisotropy of the longitudinal and transverse swelling rates of wood. *Journal of Wood Science*, *53*, 175–177.

Kuga, S., Takagi, S., & Brown, R. M., Jr. (1993). Native folded-chain cellulose II. *Polymer*, *34*, 3293–3297.

Nakagaito, A. N., & Yano, H. (2008). Toughness enhancement of cellulose nanocomposites by alkali treatment of the reinforcing cellulose nanofibers. *Cellulose*, *15*, 323–331.

Nakano, T., Sugiyama, J., & Norimoto, M. (2000). Contraction force and transformation of microfibril with aqueous sodium hydroxide solution. *Holzforschung*, *54*, 315–320.

Nakano, T. (2010). Mechanism of microfibril contraction and anisotropic dimensional changes for cells in wood treated with aqueous NaOH solution. *Cellulose*, *17*, 711–719.

Nishimura, H., & Sarko, A. (1987). Mercerization of cellulose. III. Changes in crystallites sizes. *Journal of Applied Polymer Science*, *33*, 855–866.

Nishimura, H., & Sarko, A. (1991). Mercerization of cellulose. 6. Crystal and molecular structure of Na-cellulose IV. *Macromolecules*, *24*, 771–778.

Okano, T., & Sarko, A. (1985). Mercerization of Cellulose. II. alkali-cellulose intermediates and a possible mercerization mechanism. *Journal of Applied Polymer Science*, *30*, 325–332.

Pääkkö, M., Ankerfors, M., Kosonen, H., Nykänen, A., Ahola, S., Österberg, M., et al. (2007). Enzymatic hydrolysis combined with mechanical shearing and high-pressure homogenization for nanoscale cellulose fibrils and strong gels. *Biomacromolecules*, *8*, 1934–1941.

Revol, J. F., Dietrich, A., & Goring, D. A. I. (1987). Effect of mercerization on the crystallite size and crystallinity index in cellulose from different sources. *Canadian Journal of Chemistry*, *65*, 1724–1725.

Sakurada, I., Nukushima, Y., & Ito, I. (1962). Experimental determination of elastic modulus of crystalline regions in oriented polymers. *Journal of Polymer Science*, *57*, 651–660.

Shibazaki, H., Kuga, S., & Okano, T. (1997). Mercerization and acid hydrolysis of bacterial cellulose. *Cellulose*, *4*, 75–87.

Siró, I., & Plackett, D. (2010). Microfibrillated cellulose and new nanocomposite materials: a review. *Cellulose*, *17*, 459–494.

Tarashima, N., Kitano, K., Kojima, M., Yoshida, M., Yamamoto, H., & Westermark, U. (2010). Nanostructural assembly of cellulose, hemicellulose, and lignin in the middle layer of secondary wall of ginkgo tracheid. *Journal of Wood Science*, *55*, 409–416.

Wada, M., Ike, M., & Tokuyasu, K. (2010). Enzymatic hydrolysis of cellulose I is greatly accelerated via its conversion to the cellulose II hydrate form. *Polymer Degradation and Stability*, *95*, 543–548.

Wise, L. E., Murphy, M., & D'Addieco, A. A. (1946). Chlorite holocellulose, its fractionation and bearing on summative wood analysis and on studies on the hemicelluloses. *Paper Trade Journal*, *122*, 35–43.